Structures 58 (2023) 105371

Contents lists available at ScienceDirect

Structures

journal homepage: www.elsevier.com/locate/structures

Enhancing the performance of precast hybrid concrete deep beams using curved and arched designs: Experimental investigations

Qasim M. Shakir [a], Hawraa K. Hannon [a], Ehsan Noroozinejad Farsangi [b,*]

[a] Department of Civil Engineering, University of Kufa, Iraq
[b] Urban Transformations Research Centre (UTRC), Western Sydney University, NSW, Australia

ARTICLE INFO

Keywords:
Curved hybrid
Arched hybrid
Diagonal cracking
Reactive powder concrete
Compression struts
Precast deep beams

ABSTRACT

In recent years, deep beam performance improvement has garnered significant interest, leading to several proposed solutions. This study introduces and compares two new models of hybrid concrete deep beams, aiming to outperform conventional designs. Nine experimental specimens were subjected to one-point and two-point static loadings. The specimens shared identical dimensions, with an overall span of 1700 mm, width of 180 mm, and overall depth of 450 mm. Response parameters such as cracking and failure loads, failure modes, crack propagation rates, toughness, stiffness, and ductility were evaluated. Results indicated substantial enhancements compared to the conventional hybrid model. The curved model achieved a 5 % and 12 % increase in failure load under one-point and two-point loading, respectively. The corresponding enhancements for the arched model were 13 % and 20 %. Notably, toughness improvements ranged from 32 to 39 % and 97 % under two-point loading for the curved and arched models, respectively. Ductility gains were 39 % and 45 % under two-point loading and (45–57)% and 74 % under one-point loading for the respective models. The findings highlight the potential of the curved model with reactive powder concrete-normal strength concrete (RN) composition, offering increased load-carrying capacity and the possibility of using low-strength concrete for cost and weight reduction. The arched model also demonstrated significant enhancements. Changing the loading configuration from two-point to one-point resulted in reduced capacity, but the proposed models mitigated this reduction. This study contributes valuable insights into the behaviour of precast hybrid concrete deep beams, showcasing the superior performance of the proposed curved and arched models.

1. Introduction

Recent research revealed that reinforced concrete deep beams are among the topics of great interest in the practice of structural engineering. A deep beam is one that is about as deep as the span length. Tall buildings, offshore structures, and foundations can all benefit from using reinforced concrete deep beams [1]. However, the beam (Bernoulli) theory may not cover their design due to the severe disturbance of stresses that occur within these regions caused by the dominance of the shear force, and the strut-and-tie model (STM) is used instead [2–4]. Due to the heavy loading transferred by deep beams and the nonlinearity in behaviour, many studies focused on the improvement of the performance of the deep beams using several methods, including the use of prestressing technique, the inclusion of rolled steel shapes within the concrete, using the ultra-strength concrete or the hybrid beams.

Regarding the prestressing technique, Sargious and Tadros [5] studied deep beams prestressed with straight cables. It was reported that, when a beam's height exceeds its span, the bottom prestressing forces cannot completely relieve the high tensile stresses near the top face of the beam. Sargious and Dilger [6] examined the prestressed concrete (PC) deep beams with openings while taking into account the tendons' locations, the width and depth of the openings, and other variables. It was determined that inclusion opening with PC deep beams results in a structure free of cracks and offers a productive and cost-effective use of materials. Wang and Meng [7] proposed a modified STM for simply supported PC deep beams. It was reported that failure might occur as tensile splitting along the struts or as a crushing failure by excessive compressive force within the struts or at the nodal zones. Kim et al. [8] conducted a nonlinear analysis of the strength and behaviour of prestressed concrete deep beams with straight tendons. According to Burningham et al.[9], the RC deep beams repaired with post-tensioned CFRP rods produced an ultimate load capacity that was between 1.20

* Corresponding author.
E-mail address: ehsan.noroozinejad@westernsydney.edu.au (E. Noroozinejad Farsangi).

https://doi.org/10.1016/j.istruc.2023.105371
Received 7 July 2023; Received in revised form 7 October 2023; Accepted 9 October 2023

Table 1
Coding of the tested specimens.

Group	Coding	a/h	Type of deep beam	Deep beam geometry
G1	G1-RN-2P	1.2	Horizontally	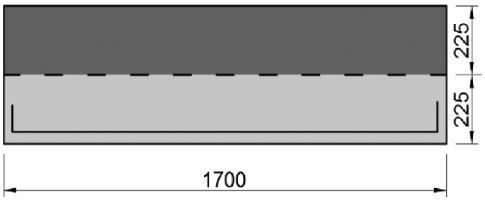
	G1-RN-1P	1.67	Hybrid	
G2	G2-RN-2P	1.2	Curved Hybrid	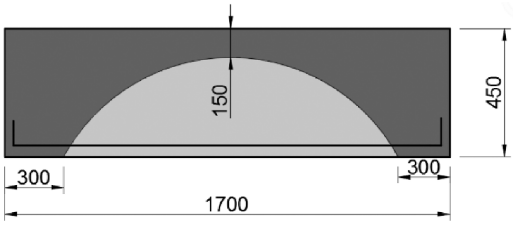
	G2-RL-2P			
	G2-RN-1P	1.67		
	G2-RL-1P			
G3	G3-NRN-2P	1.2	Arched hybrid	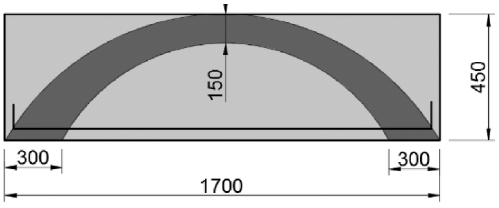
	G3-NR1N-2P			
	G3-NRN-1P	1.67		

R: Reactive powder concrete .

N: Normal strength concrete; L: Lightweight concrete .

and 1.28 times higher than their residual capacity and between 1.25 and 1.27 times higher than the control beam's capacity. Ren et al. [10] studied the flexural performance of steel deep beams reinforced by unbounded straight tendons as external prestressing. Several parameters were considered, including the influence of tendon force and variation of eccentricity on the flexural behaviour of such beams. Khalaf and Al-Ahmed [11] strengthened reinforced concrete (RC) deep beams with large openings by using externally prestressed strands of horizontal and vertical configurations. Results showed that the horizontal and vertical strengthening resulted in an overall strength gain ranging in (32–53)% and (27 %–35 %) respectively. Yang et al. [12] proposed an STM-based model to predict the ultimate load of PC deep beams. Results showed that increasing the shear capacity of beams as well as their flexural capacity, could be accomplished by using prestressing with draped configuration. Regarding the second proposal, Lu [13] suggested using an analytical technique based on the softened STM to assess the shear strengths of deep composite beams when concrete is being crushed. The results showed that the concrete strengths, shear span-to-depth ratios, and ratios of the flange width to gross width have a significant impact on the behaviour of the tested beams. Chen et al. [14] considered the deep beams composed of internal steel shape. It was determined that more ductile behaviour than the RC deep beams was obtained, and that the wide flange shape may significantly contribute to the shear strength of the steel-reinforced concrete (SRC) deep beams. It was also determined that the depth of the wide flange shape may affect the shear strength of the SRC deep beams.

For the high-performance (or SFC) concrete, Fahmi et al. [15], investigated the behaviour of reactive powder concrete (RPC) deep beams with compressive strengths of (95–111) N/mm^2 and subjected to concentrated loads. It was concluded that the shear strength increased by 24.4 and 31.7 % when the a/d ratio decreased from 1.5 to 1.25, and 1.0, respectively. Ma et al. [16] conducted an experimental study on the effectiveness of HFRC using two different types of steel fibers with a strength range of (80–103) N/mm^2. The ratio of web reinforcement and the volume fraction of steel fibers were the main factors. According to reports, diagonal cracks formed during the construction caused all of the beams to fail. Moreover, it was obtained that the ultimate load improved in the range (66.8–114.2)%, respectively. In 2018, the behaviour of deep beams made of hybrid steel-polypropylene fiber-reinforced high-performance concrete (HFRHPC) with concrete strength (88–114) N/mm^2 was studied experimentally and analytically by Smarzewski [17]. It was obtained that capacity improved by 28 %, with the content of polypropylene fibre increased from 1 % to 1.5 % and steel fibre was increased from 0.05 % to 0.1 %. Dang etal. [18] concluded that using steel fibers in deep beams reduced shear crack width by up to 68 percent, increased shear resistance of deep beams by up to 55 percent, decreased displacement of beams by up to 57 %, and increased shear beams' capacity for deformation by up to 45 percent. Chen et al. [19], concluded that the shear strength is affected positively with reducing (a/h) and increasing other variables. Additionally, it was stated that deep beams

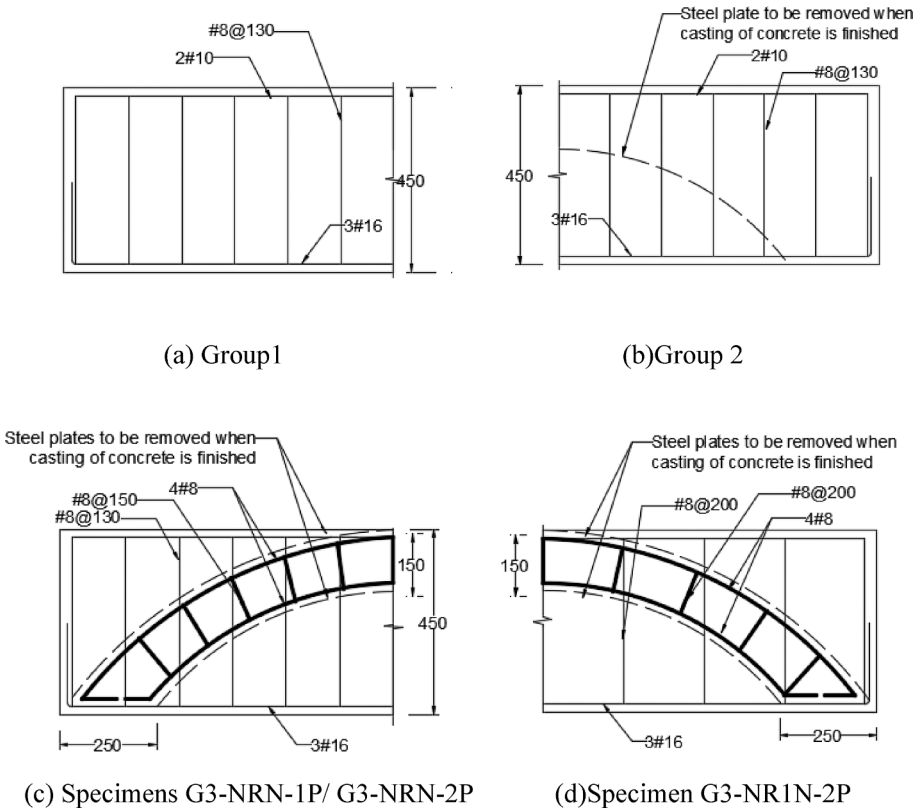

Fig. 1. Details of Reinforcement the tested specimens.

were dominated by the "beam action" prior to load levels of 50 % to 70 %; following that, they were dominated by the "arch action". Sagi et al. [20] studied The shear behaviour of self compacting concrete (SCC) RC deep beams with macro steel fibers of (0.5 %,1.0 %, and 1.5 %). Test results showed that adding fibers greatly increased the first cracking load, ultimate shear capacity, ultimate deformation, and ductility. However, the ultimate shear capacity was not increased by the addition of steel fiber at a volume fraction greater than 1.0 %.

Regarding the hybrid concrete deep beams, the conventional model that consisted of two horizontal layers, top with high-strength concrete (HSC) and the bottom with normal strength concrete (NSC) was proposed [21–23]. However, only the top nodal points are included in the HSC layer, and the strength of the bottom layer generally controls the behaviour of the beams. Thus, no significant improvements were reported.

Based on the above discussions, it can be observed that the prestressing technique has several advantages, including the higher capacity and elimination of the effect of shear. There are several issues that restrict the wide use of this technique, such as the high cost, advanced technology, and the fact that high-strength concrete is needed to make use of the high strength of the prestressing strand. For the deep beams with embedded steel shape, there are two issues that arise as an obstacle to gaining high performance, which are the bond slip and separation between the steel section and concrete. Moreover, buckling of the steel shape may control the failure of the composite deep beam. For the UHP and SFC deep beams, the high cost of the constituent materials combined with the large dimensions of the deep beams restricts the use of such models widely. For the horizontal hybrid deep beam, two layers of concrete are used. One layer with UHPC/SFC and the other with NSC. This model was controlled by failure at the nodal zones and parts of the compression struts.

Shakir and Hannon [24] proposed a new model of precast hybrid concrete deep beams with SFC at the top layer only. The model was based on the curved distribution to optimize using the types of concrete within successive sections of the beam instead of the conventional hybrid model. Two systems of loadings were considered: one mid-span and two-third point loads. Results revealed that for the two systems (one point-two points), capacity improved, relative to the control beams, by (23 % – 27 %) and (23 % – 32 %) for the two models, respectively. Shakir and Hannon [25] used the RPC in the top layer instead of steel fiber concrete (SFC). According to the results, the capacity of the two models increased by 27.6 % and 39 %, respectively, under one-point loading. For tests under two-point loads, the respective enhancements in capacity were 34 % and 36.9 %. Shakir and Hannon [26] proposed the arched hybrid model with SFC along the strut elements. Results revealed the ultimate load improved, by 45 %, with a reduction of 5 % for specimens under a one-point load. Additionally, it was reported that switching from normal-weight concrete to lightweight concrete under the curved interface line resulted in a 1 % reduction in capacity for both systems of loading.

In the present work, A more advanced hybrid model compared to previous studies has been proposed, which is called an "arched model" due to the formation of a strong arch of the concrete of relatively high strength along the major path of load transfer. Comparisons between the two models have been made considering the cracking load, failure load, maximum deflection, map of crack propagation, crack width, resilience, toughness, stiffness, ductility, volume of the concrete mixes and mode of failure. The suggested model might lead to a decrease in production costs of deep beams and in a more advanced stage, to produce lightweight and sustainable concrete deep beams or conventional beams with acceptable shear and B.M. capacity.

2. Experimental work

2.1. Description of specimens

Nine hybrid concrete deep beams with dimensions of 180 mm in width, 450 mm in depth, and 1700 mm in length (with a c/c span of

Table 2
Material constituents of the concrete mixes.

Materials	RPC	LWC	NC
Cement (kg/m^3)	900	400	470
Natural sand (kg/m^3)	–	650	837
Gravel (kg/m^3)	—	–	800
Silica sand (kg/m^3)	900	–	
L W A (Leca) (kg/m^3)	–	400	–
Steel fiber (kg/m^3)	117	–	–
Silica fume(kg/m^3)	225	8	–
Lime stone(kg/m^3)	–	–	99
Water(l/m^3)	253	146.88	159.32
Superplasticizer(l/m^3)	28	6.53	7.52

Table 3
Properties of concrete mixes.

Type of mix	Compressive strength (MPa)		Indirect tensile strength(f_t) (MPa)	Elastic modulus (E)GPa
	Cube (f_{cu})	Cylinder(f 'c)		
RPC	93	76	9.0	39.3
NSC	46	37	2.4	27.4
LWC	37	31	2.3	24.3

1500 mm) are tested experimentally under a scheme of static loading that is gradually increased up to failure. The specimens are grouped according to the model of hybridization, as shown in Table 1. Group 1 (G1), which represented the conventional hybrid model, included two specimens, one with a/h = 1.2 (two-point loading) and the other with a/h = 1.67 (under one mid-span loading). The second group G2, which represents the curved hybrid model, consisted of four specimens, two are hybrid with NSC or LWC at the bottom layer of the beam, considering the value of a/h for the specimens symmetrically. The region above the curve interface was made of RPC. The third group G3, which consisted of RPC within the strut region and NSC at other regions, represents the proposed arched model consisting of two specimens, one with a/h = 1.2 and the second with a/h = 1.67. All nine specimens included shear reinforcement in the form of vertical stirrups. In the specimen G3-NR1N-2P, which is tested under two point loads (a/h = 1.2), the spacing of stirrups in both beam and struts was increased to 200 mm to study the effect of reducing the shear reinforcement on the behaviour. Three types of concrete mixes were used to produce the proposed model of hybrid concrete deep beams. These types include mixes for reactive powder concrete (RPC), normal strength concrete (NSC), and lightweight concrete (LWC). Steel reinforcement used consisted of three sizes. #8 was used in stirrups and ties of the arch (in group 3), #10 as the top reinforcement of the beams and #16 as tie reinforcement at the bottom part of the tested beams. In Table 1, the coding of the specimens is provided as (Gn-XX-mP). The first parameter refers to the group number (n = 1,2,3), while the second part refers to the hybridization model, which is either RN or RL for groups G1 and G2. For group G3, this part is either NRN or NR1N. The third part refers to the type of loading, which is either midspan point loading (1P) or two-point loading (2P). The detailing of steel reinforcement for the tested specimens has been shown schematically in Fig. 1.

2.2. Materials

In the experimental work, ordinary Portland cement has been used. To ensure compliance with Iraqi Specification No. 5, 1984 [27], the results of chemical and physical analyses are evaluated. The mixing and curing of the deep beam specimens were done using tap water (W). The fine aggregate (FA) and coarse aggregate are tested according to the Iraqi Specification No. 5 & 45, 1984 [28,33]. The lightweight concrete mix has a maximum aggregate size of 8 mm and is provided using lightweight aggregate (Leca). Silica sand with a maximum particle size of 0.6 mm was used in reactive powder concrete mix. To improve the particle packing of the concrete and to increase its performance, high-performance concrete mixes use silica fume, mega Add MS(D). Glenium 54, a Superplasticizer, has been used in concrete mixtures to reduce the amount of water, produce concrete with very high early and ultimate strengths with few voids, and increase workability without segregation or bleeding. It is a component of every concrete mix. The shear resistance and durability of the reactive powder concrete mix have been improved by the use of straight micro steel fibers with a diameter of 0.22 mm and a length of 13.1 mm.

The yield stress for the three bar sizes (#8 mm, #10 mm & #16 mm) were 445 N/mm^2, 480 N/mm^2, and 600 N/mm^2, respectively. The respective tensile strengths were 630 N/mm^2, 695 N/mm^2, and 697 N/mm^2. Materials were examined in the testing laboratory at Kufa University's Engineering Consultant Office. Table 2 indicates the proportions of the constituent materials of the concrete mixes used in the present study. Furthermore, the tests of compressive and tensile strengths of the three mixes are shown in Table 3.

2.3. Casting of specimens

The steel reinforcement was installed after the preparation of the plywood forms, Fig. 2a. The steel plate that separates the two types of concrete was then fixed inside the forms, as depicted in Fig. 2b. The three types of concrete were prepared simultaneously using two mechanical mixers, and cast into the forms on both sides of the steel plates at the same time. The separating plates are removed as soon as the casting process is complete. To maintain humidity and temperature, burlap sacks and plastic sheets are placed over the warm water curing stage for the cubes, cylinders, and beams. The specimens are shown in Fig. 2c and Fig. 2d after the separating steel plates have been removed, while Fig. 2e shows the hardened specimens after painting according to type of concrete (see Table 1). The steps of mixing the three concrete mixes are depicted in Fig. 3.

2.4. Testing setups and response measurements

The 200-ton testing machine shown in Fig. 4a was used to apply a central static load that was gradually increased until failure. While the load and deflection values were recorded using the data logger depicted in Fig. 4b. Utilizing (LVDT), the mid-span deflection was measured. Additionally, a crack meter was used to measure cracks up to 0.5 mm in width. In contrast, widths greater than 0.5 mm were measured using a digital Vernia.

The measuring devices used in this study are displayed in Fig. 5. Two specimens that are tested with a two-point load are shown in Fig. 6.

3. Results and discussions

3.1. Map of crack propagation

Fig. 7a displays the map of crack propagation for specimen G1-RN-2P. With an 80 kN loading stage, a flexural crack first appeared at the mid-span maximum B.M. region. As the load increased, cracks grew larger and more started to form on both sides. At a load of 300 kN, cracking at the junction between the regions of max. moment and max. shear developed. It can be observed that the highly restrained cracks at the RPC layer due to steel fibers resulted in the propagation of cracks laterally, leading to significant curvature of the beam. More cracks initiated and developed within the shear span and oriented to the loaded points. Again, due to the RPC at the top layer, cracks could not reach the compression fiber. Test was terminated by semi-diagonal cracks accompanied by significant crushing at the supports.

Failure can be seen to be influenced by a number of factors, including:

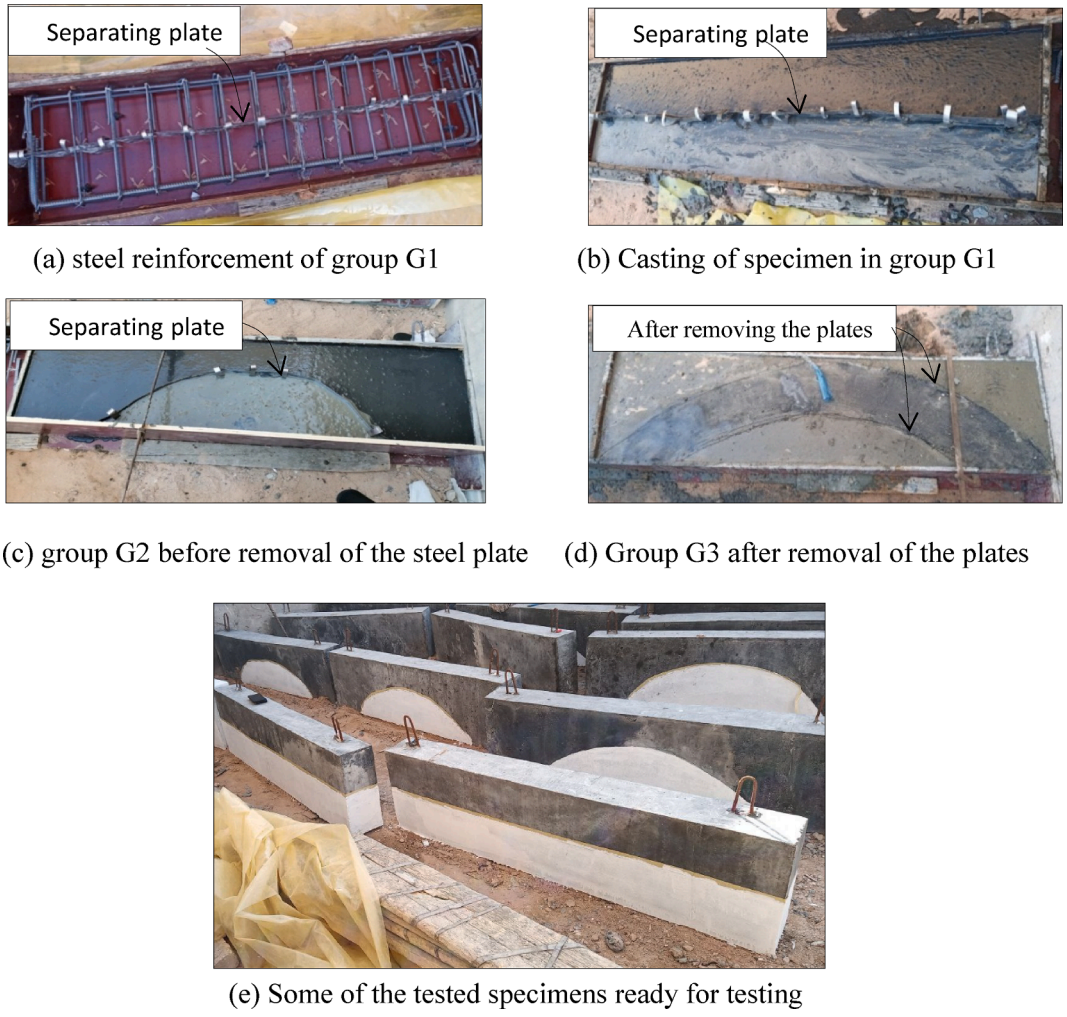

(a) steel reinforcement of group G1

(b) Casting of specimen in group G1

(c) group G2 before removal of the steel plate

(d) Group G3 after removal of the plates

(e) Some of the tested specimens ready for testing

Fig. 2. Formwork and casting of the hybrid deep beams.

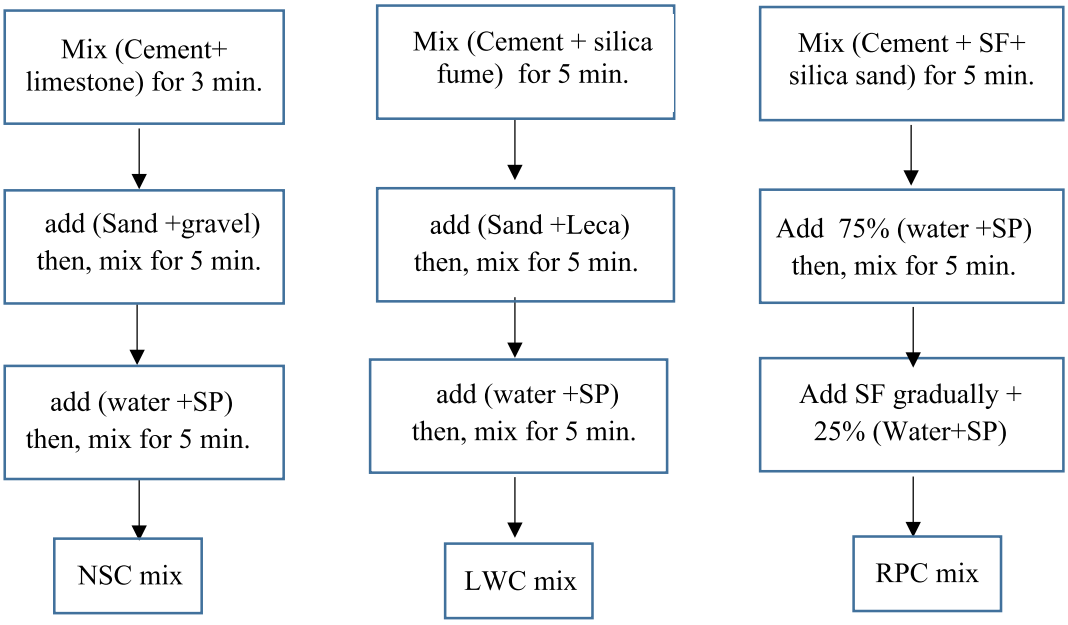

Fig. 3. Steps for preparing the mix types used in the present study.

(a) loading machine (b) data logger

Fig. 4. Testing Machine.

Fig. 5. Response measuring tools.

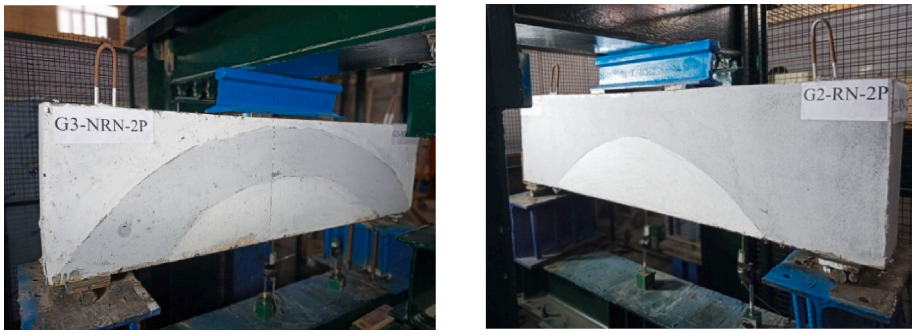

Fig. 6. Specimens under two-point testing.

1- Tensile strength that is normal to the diagonal lines connecting the loading point to the supports. This is maintained partially by the shear reinforcement of deep beams, which is represented in this beam by the vertical stirrups.
2- The dimensions of the ideal compressive elements such that there is enough cross-sectional area that could resist compressive forces without buckling. This is also achieved by the steel crossing the compression element (compression struts).
3- Strength of the top nodal points such that no crushing occurred at such points due to severe loading. Strength of the bottom nodal points such points represent (CCT).

(a) specimen G1-RN-2P

Fig. 7. Cracking patterns of specimens tested under two-point loads.

4- the strength of the tie connecting the bottom nodal points. If strength is not efficient, premature failure may occur.

Thus, the proposed model focused on providing an efficient path for stress transfer, strength and bearing capacity.

The first model was called the "curved model" due to the curved interface line between the two layers. It can be seen from Fig. 7b that for the composition RPC-LWC, cracks developed with the LWC region. The rate of propagation out of the region is very few, due to the high resistance of the RPC layer to cracking. However, the first crack that initiated at midspan developed vertically with a slow rate up to reaching the compression fibre. At load 60, failure occurred by flexure mode compared to specimen G1-RN-2P, which failed by semi-flexural cracking. It is clear that the curved model, as opposed to the traditional hybrid model, shifted the failure to be a flexural failure or more ductile.

For specimen G2-RN-2P, Fig. 7c, the strength of concrete under the curved line was increased, and NSC was used instead of LWC. It can be observed that No. the cracks and penetration towards the compression face reduced and became relatively slow due to the energy dissipated within the NSC layer. It is to be mentioned that some unbalance at the final stages of loading occurred caused by non-perfectly symmetric cracking due to nonhomogeneous concrete material. The mode of failure was shifted slightly to be closer to that of specimen G1-RN-2P rather than of specimen G2-RL-2P.

It can be seen that no significant difference in cracking pattern occurred. This may be attributable to the small differences between the tensile strengths and the concrete at the regions below the neutral axis in which its resistance is neglected. From another side and based on the arching action, these parts are out of the effective area that contributes to the resistance, as shown in Fig.(7c). Thus, changing the type of concrete did not affect the general behaviour of the beams. This is a very important issue in optimization studies of structural members. i.e. determining the optimum distribution and selection of suitable materials according to the type and intensity of stresses induced in the section. Then the cost and weight of precast members may be reduced.

Moreover, waste of construction materials that have low compressive strength, such as crushed concrete, bricks, tiles, thermos stone, etc. may be used as a coarse aggregate in concrete to fill such parts out of the path of stress transfer. This will result in reducing the environmental effect of these wastes and reduce the cost of construction as well as reducing the weight of the members for lightweight wastes. It is to be mentioned that the top corners for specimens G1-RN-2P, G2-RL-2P and G2-RN-2P are free from cracking. i.e. from effective stresses. Because such regions are out of the arching action and path of transfer of stresses. Thus, it is expected that removing (neglecting) or reducing the strength of these regions may not seriously affect the capacity of the beam, keeping in mind that an efficient load transfer to the arch should be provided.

Fig. 7d shows the cracking pattern for the second proposed hybrid (arched) model for deep precast beams by which the RPC was used only within the compression strut (or region of effective arching action). As can be seen, the additional reinforcement of the arch significantly slowed the growth of cracking both vertically and inside the arch.

It is expected that the additional reinforcement in the arch of the hybrid concrete deep beam may contribute significantly to the shear resistance of the beam and may substitute some of the resistance provided by the vertical stirrups. In Specimen G3-NR1N-2P, the spacing of both stirrups of the beam and ties of the arch is increased from 150 mm to 200 mm, i.e. an increase of 30 %. Fig. (7e) shows the cracking pattern for the specimen, and it is obvious that the diagonal cracking appeared to be clearing within the HPC arch, referring to a reduction in shear strength on the beam.

Fig. 8a to d present the cracking pattern for the corresponding specimens under midspan concentrated loads (except for specimen G3-NR1N-2P). It is aimed to check the efficiency of the various models of hybridization to resist the applied loading under short-term static load.

Comparing specimen G1-RL-1P with G1-RL-2P, it is obvious that the conventional hybrid model may not transfer the applied load effectively as in the curved or the arched models. it is clear that the reduction in load capacity for the conventional model was 30 %, while for the curved model, the reductions were 25 % and 23 % for the compositions RPC-NSC and RPC-LWC, respectively, with increments in failure loads for the one-point system of 12 % and 10 % respectively. For the second hybrid model, the effect of the arch in providing an efficient path to transfer the load to supports and prevent localization of stresses. Results revealed that the reduction in capacity due to changing the system of loading was 25 %, with an increment in failure load for the one-point system relative to the conventional hybrid model by 20 % and max. deflection by 63 %. Table 3 shows how changing the loading system affects the failure load and maximum deflection.

3.2. Load-deflection curves

The effect of the hybrid model on the history of loading for the hybrid concrete deep beams tested under two-point loading is shown in Fig. 9. The conventional model produced the lowest deflection at failure, as can be seen. Regarding the first proposed model (curved model), an enhancement in load capacity by (0 %) and (5 %) were obtained when adopting the composition RPC-LWC (specimen G2-RL-2P) and RPC-NSC (specimen G2-RN-2P), respectively. It can be observed that there is no reduction in failure load and max. deflection increased when adopting

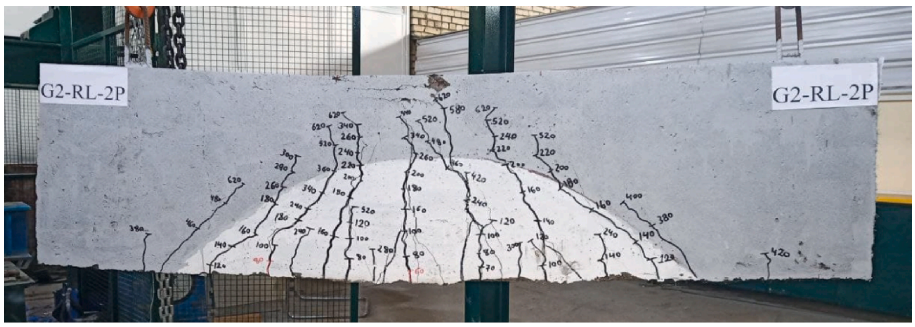

(b) specimen G2-RL-2P

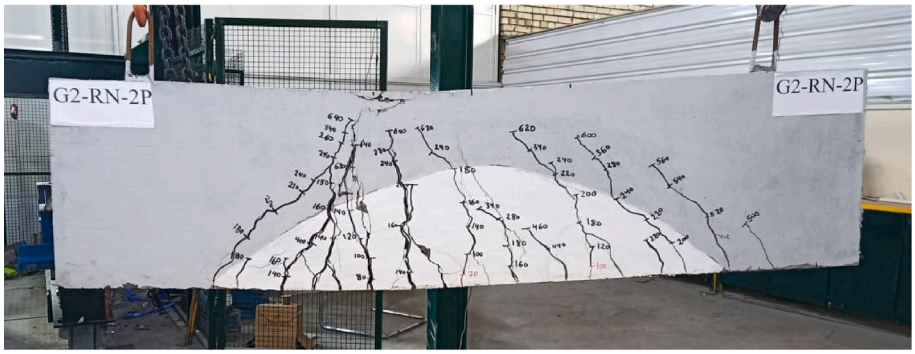

(c) specimen G2-RN-2P

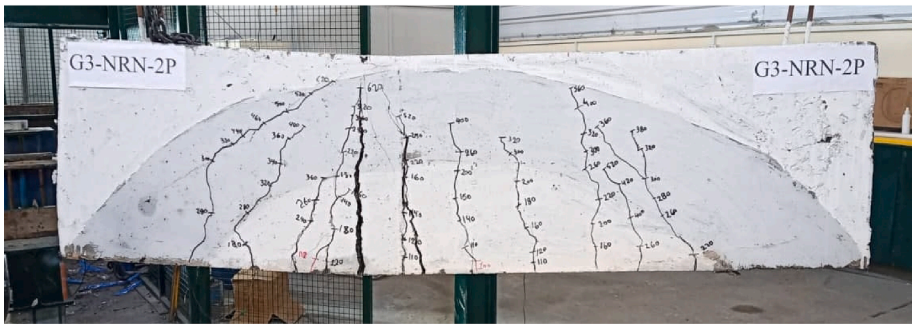

(d) specimen G3-NRN-2P

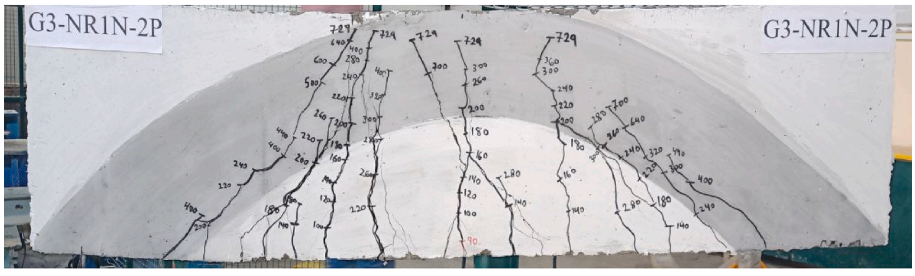

(e) Specimen G3-NR1N-2P

Fig. 7. (*continued*).

the composition RPC-LWC rather than RPC-NSC. i.e. (32 %) and (24 %) respectively. This may be important in the production of lightweight or sustainable full-scale members by using recycled aggregate from crushed concrete or other construction materials.

When adopting the second proposal (arched model), it can be seen that a significant improvement in load and deflection at failure were (13 %) and (38 %). Then, it can be concluded that using some reinforcement within the compression strut has two main roles:

1- Improving the stress transfer through the struts, which acted as a tied arch and controlled the tensile stresses, occurred at the lower parts of the arch due to the buckling of the strut out of its central plane.

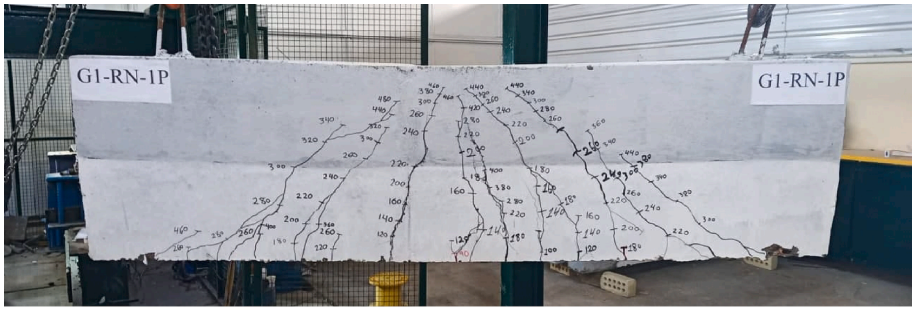

(a) specimen G1-RN-1P

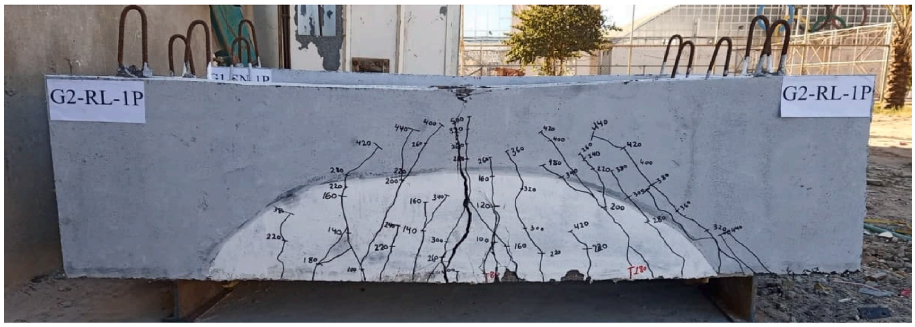

(b) Specimen G2-RL-1P

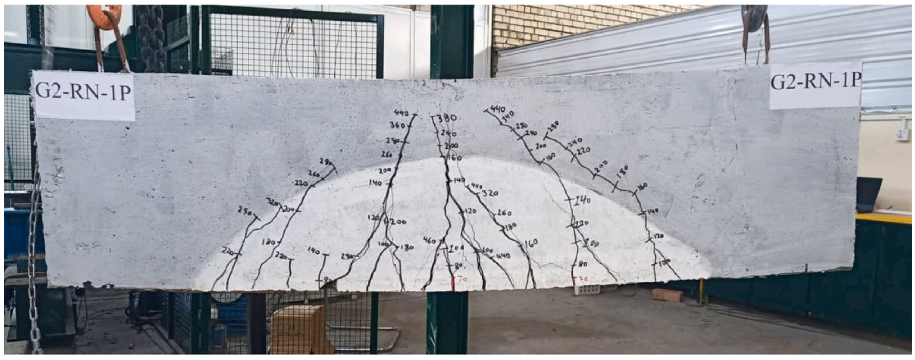

(c) Specimen G2-RN-1P

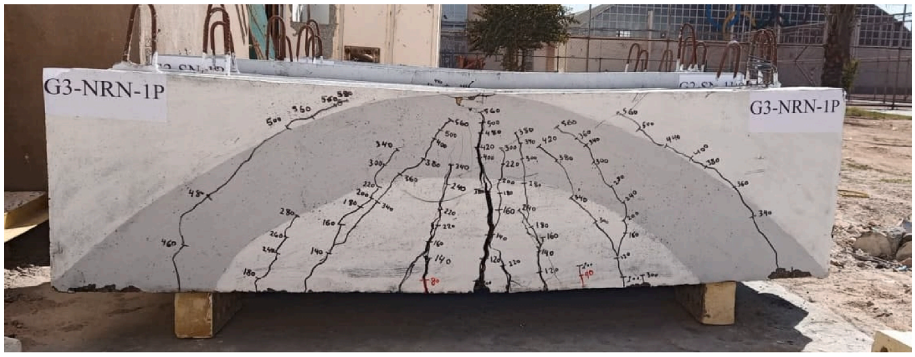

(d) Specimen G3-NRN-1P

Fig. 8. Cracking patterns of specimens tested under one-point loads.

2- reducing the effect of the tensile stress normal to the path of the diagonal shear, which generally occurs parallel to the compression strut, and then improve the efficiency of the bottled-shaped strut.

For the proposed configuration of increasing the spacing of the stirrups from 130 mm to 200 mm, it can be seen that stiffness is reduced by 31 % relative to the specimen G3-NRN-2P. At the same time, a significant reduction in maximum deflection can be observed. This may be attributed to increasing the spacing of stirrups, which might reduce the quantity of shear reinforcement that crosses the diagonal crack. And then, reducing the resistance to diagonal cracking. Consequently, it may be concluded that ties in the arch may not substitute the increase in spacing between shear reinforcement, and such ties act mainly to restrict the buckling of the longitudinal reinforcement of the arch.

Fig. 10 shows the results of the hybrid concrete deep beams tested under midspan point loading. It is clear that the conventional hybridization arrangement yielded the smallest load capacity and deflection at failure. When using the curved hybrid model with the composition RPC-

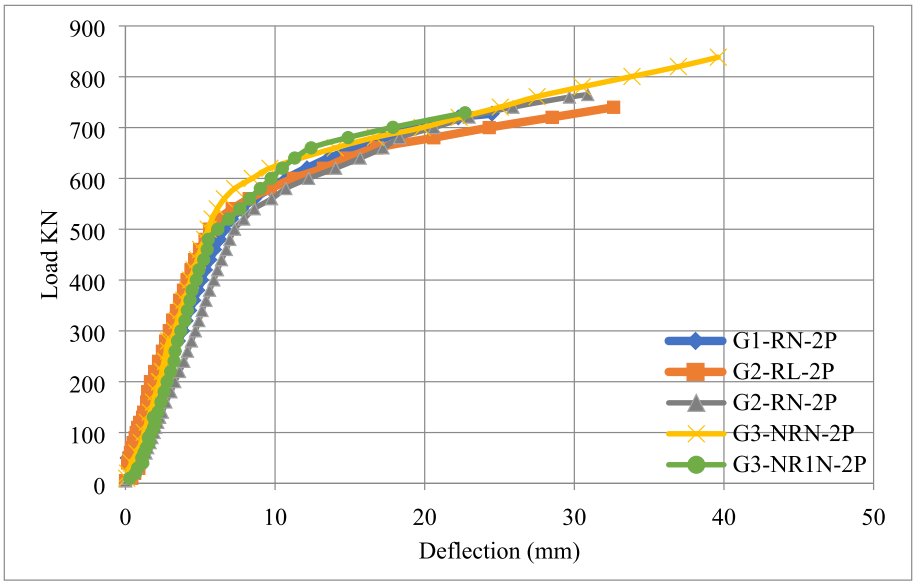

Fig. 9. Load–deflection curves for hybrid deep beams under two-points loading.

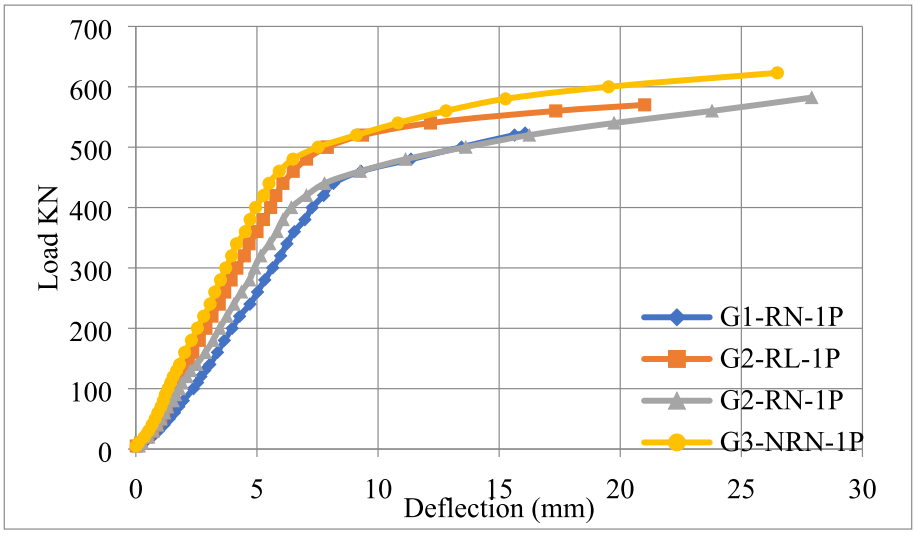

Fig. 10. Load–deflection curves for hybrid deep beams under one-point loading.

Table 4
Failure loads and maximum deflections of the hybrid deep beams.

Specimen	Two-points		One-point		ΔP	Δd
	Load (Δ%)	Def. (Δ%)	Load (Δ%)	Def.(Δ%)		
G1-RN-	740(0)	25(0)	520(0)	16(0)	−30 %	−36 %
G2-RN-	780(5 %)	31(24 %)	582(12 %)	28(+75 %)	−25 %	−10 %
G2-RL-	740(0)	33(32 %)	570(10 %)	21(+31 %)	−23 %	−36 %
G3-NRN-	838(13 %)	40(38 %)	623(20 %)	26(+63 %)	−25 %	−35 %
G3-NR1N-	730(−1 %)	23(−8 %)				

LWC resulted in an enhancement in failure load and maximum deflection of 10 % and 31 %, respectively. For the composition RPC-NSC, enhancements of 12 % and 75 % for failure load and the corresponding deflection, respectively, were recorded. For the arched hybridization configuration, improvements of 20 % and 63 % were obtained. It can be observed that adopting the LWC instead of NSC resulted in reducing the max. deflection only. Consequently, some reductions in toughness and ductility occurred. Moreover, it is clear that both systems of loading the RPC-LWC resulted in higher stiffness compared to the RPC-NSC. This effect may be attributed to the difference in a stage when the arching action controlled the behaviour, which occurs earlier in RPC-LWC than RPC-NSC.

The general behavior is significantly influenced by the loading system, as evidenced by a comparison of the results in Figs. 9 and 10. For the conventional hybrid concrete deep beams, it is obvious that the deflection reduced from 25 mm to 16 mm and the corresponding load reduced from 740 kN to 520 kN, i.e. reductions by 30 % and 36 % were recorded when adopting the one-point rather than the two-point loading. For the first hybrid model, it was found that a reduction of 25 % and 10 % in failure load and deflection for the composition RPC-LWC. While the reductions were 23 % and 36 % for the composition RPC-NSC. For the second proposal, reductions of 25 % and 35 % were

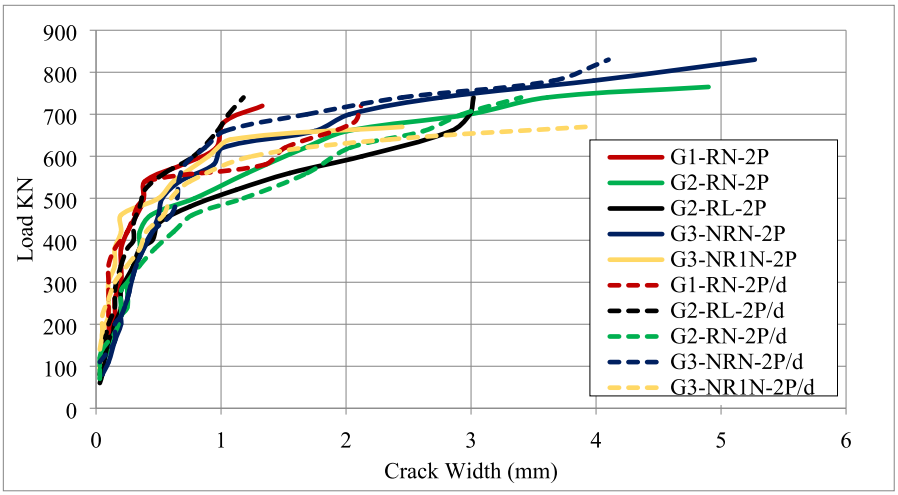

Fig. 11. Crack width of the hybrid specimens-two point loads.

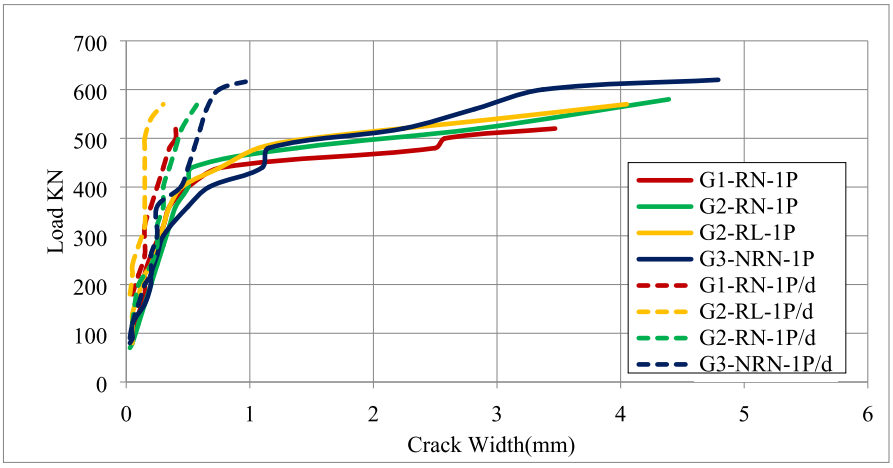

Fig. 12. Crack width of hybrid specimens-one point load.

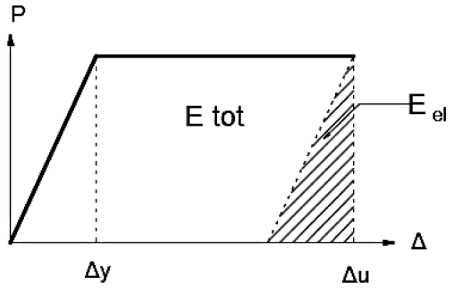

Fig. 13. Calculating the ductility ratio using the method of dissipated energy [32].

recorded when adopting the one-point rather than the two-point system. All the test results of the hybrid concrete deep beams are depicted in Table 4.

3.3. Crack width

The rate of crack widening for the specimens tested under two-point loading is shown in Fig. 11. For the traditional hybridization model G1-RN-2P, it can be seen that the width of the flexural crack increased quickly in comparison to the diagonal one. Due to the spread of additional cracks throughout the specimen's body, the flexural crack eventually stagnated. Results for specimen G2-RN-2P showed that the diagonal crack's width is greater than the flexural crack's width up to a load of 700 kN (more than 90 % of the total loading history). Beyond this, the flexural crack widened rapidly due to the resistance at the arched interface to the diagonal cracking. As can be seen, the arching effect controlled the final stages for the two specimens, resulting in the failure of the flexural type. For the G3-NRN-2P model, both the diagonal and flexural cracks are close to each other. At high loading stages, the width of cracks expands rapidly, so that the width of the flexural and diagonal cracks is 5.27 mm and 4.21, respectively. For G3-NR1N-2P specimen, which included reduced shear and tie reinforcement by 30 % relative to G3-NRN-2P. It can be seen that the diagonal cracks started to develop more than the flexural cracks after loading 340 kN, and the specimen failed with diagonal failure.

Fig. 12 displays the rate of crack enlargement as loading progresses for specimens tested under one point load and including RPC. It is obvious that the flexural cracks are widening at a faster rate than the diagonal ones. This might be a result of the STM design method's recommendation to use a minimum amount of steel to cross the compression strut. This type of steel acts as shear reinforcement, meaning that using more steel than is necessary could cause the deep beam to fail by flexural mode. Furthermore, it can be seen that up to a

Table 5
Values of Toughness, Stiffness and Ductility of the tested specimens.

Specimens	Toughness (kN*mm)	(ΔT)% Toughness Ratio	Stiffness, K (kN/mm)	ΔK%	Ductility (μ)	Δμ%
G1-RN-1P	5627	–	58.6	–	1.66	–
G2-RL-1P	9030	60	73.8	26	2.406	45
G2-RN-1P	11,933	112	60	2	2.598	57
G3-NRN-1P	12,587	124	85	46	2.883	74
G1-RN-2P	12,731	–	*74.2	–	2.289	–
G2-RL-2P	17,713	39	*89.3	20	3.182	39
G2-RN-2P	16,824	32	*69.4	−6	2.389	4
G3-NRN-2P	25,047	97	*84.8	14	3.327	45
G3-NR1N-2P	12,357	−3	58.8	21	2.516	10

load of 400 kN, the two arched hybrid models, G2-RL-1P and G2-RN-1P produced the same rate of flexural crack widening. When RPC was used on the G3-NRN-1P specimen, it was found that the cracks quickly widened and did so more quickly than on the previous specimens. The crack width of the diagonal cracks develops for two-point loads loading more than the ones tested under concentrated load. It is to be mentioned that the continuous lines represent the width of the flexural crack. While, the dotted lines represent the width of the diagonal crack.

3.4. Flexural toughness, stiffness and ductility

The ability of a member to resist deflections before failing is measured by its flexural toughness [29,30]. The area under the load–deflection curve at stiffness equal to or greater than zero serves as a representation of it. As a result, the member gradually loses the energy it produces until failure.

The stiffness K of a body represents the degree to which an elastic body resists deformation. The "effective secant stiffness" was used, based on strength at the service load stage of 0.75*Pu, [31]. Consequently, the effective stiffness K_e can be calculated using equ.1:

$$K_e = \frac{0.75P_u}{\Delta_{0.75P_u}} \quad (1)$$

The ability to withstand inelastic deformation without reducing the maximum load until failure is referred to as ductility [32]. High ductility structural members frequently withstand high deformations before failing. According to Fig. 13, the calculation was based solely on the energy dissipation that occurred during the elastic stage and throughout the entire history of loading. The ductility ratio can then be written as follows:

$$\mu = 0.5(1 + \frac{E_{tot}}{E_{el}}) \quad (2)$$

$\mathbf{E}_{tot}$. is the entire amount of energy was lost before failure, which is represented by the full area under the load–deflection curve,
$\mathbf{E}_{el}$. Predicted energy dissipation only occurs during the elastic stage of loading (area of the hatched triangle); Δy and Δu are the deflection at the yielding point (taken corresponding to the service load stage) and ultimate load. The calculated toughness, stiffness and ductility of the tested specimens are shown in Table 5.

4. Conclusions

In the present study, two new models of hybrid concrete deep beams are proposed and compared with the results of the conventional (Horizontal) hybrid deep beam. Nine experimental specimens were subjected to static loading up to failure. Two systems of loading are considered, which are one-point and two-point loadings. Through the study conducted on the hybrid concrete deep beams, the main conclusions drawn from the results of the experimental work are listed below:

1- The proposed curved model using the RN composition resulted in improving the capacity by 5 % and 12 % for the one-point and two-point loadings, respectively. For the RL composition, the corresponding values were 0 % and 10 %. This means that it is possible to use low-strength concrete in place of the LWC to reduce cost, and weight and to produce sustainable structure. Regarding the arched model improved that capacity by 13 % and 20 % for the one-point and two-points, respectively.
2- Changing the system of loading from two points to one point may result in reducing the capacity by 30 % for the conventional model. While, for the two proposed modes, the enhancements were (23–25) % and 25 %, respectively.
3- Regarding toughness, an enhancement in the range (32–39) % was obtained for the first proposed model under 2-point loading. While enhancement of 97 % for the arched model. for the one-point, the corresponding values were (60–112)% and 124 %.
4- Effective stiffness improved by 20 % (as max.) for the RL-composition. Whereas for the arched model under one-point and two-point loads, the corresponding values were 26 % and 46 %, respectively.
5- Ductility for the two-point loading was improved by 39 %, whereas for the arched model, the improvement was 45 %. The corresponding values for the one-point loading, were (45–57)% and 74 %.
6- The proposed models improved the failure to be more ductile, and the mode of failure was shifted from diagonal shear cracking with some crushing at supports (for the horizontally hybrid model) to the flexural mode of failure. This change in behavior is necessary to improve the safety of the precast deep beams.
7- This study presented two proposals for precast deep beams with lower cost and less weight. More ductile and stiffer behavior was obtained. The first proposal (curved hybrid) may be used with prestressed deep beams as it provided ends with high strengths, which may provide adequate support for seating the anchorage of the post-tensioned strands. Moreover, it may be used with prestressed and non-prestressed deep beams produced by the segmental procedure.

Funding

The authors received no specific funding for this work.

Declaration of Competing Interest

The authors declare that they have no known competing financial interests or personal relationships that could have appeared to influence the work reported in this paper.

References

[1] Shakir QM, Al-Sahlawi YM, Abd BB, Hamad SA. Nonlinear Finite Element Analysis of High-strength Reinforced Concrete Beams with Severely Disturbed Regions. Jordan J Civ Eng 2023;17(1):23–33. https://doi.org/10.14525/jjce.v17i1.03.
[2] Shakir QM, Alsaheb SDA. High strength self-compacting corbels retrofitted by near surface mounted steel bars. Pollack Period 2022. https://doi.org/10.1556/606.2022.00664.

[3] Sarah A Hamad, "Behaviour of RC Beams with Strengthened Web Openings under Vertical Loads 2021 IOP Conf. Ser.: Mater. Sci. Eng. 1094 012062, 10.1088/1757-899X/1094/1/012062.
[4] Zhang Y, Zhang S, Li T, et al. Cyclic response and shear mechanisms of RC short walls strengthened with engineered cementitious composites thin layers. Archiv Civ Mech Eng 2023;23:148. https://doi.org/10.1007/s43452-023-00683-x.
[5] Sargious MA, Tadros G. Stresses and Forces in Deep Beams Prestressed with Straight Cables. PCI J 1974;19(4):86–99.
[6] Sargious M, Dilger W. Prestressed Concrete Deep Beams With Openings. PCI J/ May-June 1977;22(3):64–79.
[7] Wang GL, Meng SP. Modified strut-and-tie model for prestressed concrete deep beams. Eng Struct 2008;30(12):3489–96. https://doi.org/10.1016/j.engstruct.2008.05.020.
[8] T.H. Kim, J.H. Cheon, H.M. Shin, Evaluation of behaviour and strength of prestressed concrete deep beams using nonlinear analysis, vol. 9, no. 1, pp. 63–79, 2012.
[9] Burningham CA, Pantelides CP, Reaveley LD. Repair of reinforced concrete deep beams using post-tensioned CFRP rods. Compos Struct 2015;125:256–65. https://doi.org/10.1016/j.compstruct.2015.01.054.
[10] Y. Ren, Y. Wang, B. Wang, H. Ban, J. Song, and G. Su, "Flexural behaviour of steel deep beams prestressed with externally unbonded straight multi-tendons," Thin-Walled Struct., vol. 131, no. September 2017, pp. 519–530, 2018, doi: 10.1016/j.tws.2018.07.022.
[11] Khalaf MR, Al-Ahmed AHA. Shear strength of reinforced concrete deep beams with large openings strengthened by external prestressed strands. Structures 2020;28:1060–76. https://doi.org/10.1016/j.istruc.2020.09.052.
[12] T. Y. Yang, A. A. Dashlejeh, A. Arabzadeh, and R. Hizaji, New model for prediction of ultimate load of prestressed RC deep beams, Structures, vol. 23, no. August 2019, pp. 509–517, 2020, doi: 10.1016/j.istruc.2019.12.014.
[13] Lu WY. Shear strength prediction for steel reinforced concrete deep beams. J Constr Steel Res 2006;62(10):933–42. https://doi.org/10.1016/j.jcsr.2006.02.007.
[14] Chen CC, Lin KT, Chen YJ. Behaviour and shear strength of steel shape reinforced concrete deep beams. Eng Struct 2018;175(February):425–35. https://doi.org/10.1016/j.engstruct.2018.08.045.
[15] Fahmi HM, AlShaarbaf IAS, Ahmed AS. Behaviour of Reactive Powder Concrete Deep Beams. AL-Mansour J 2013:1–22.
[16] K. Ma, T. Qi, H. Liu, and H. Wang, Shear behaviour of hybrid fiber reinforced concrete deep beams, Materials (Basel)., vol. 11, no. 10, 2018, doi: 10.3390/ma11102023.
[17] P. Smarzewski, Analysis of failure mechanics in hybrid fibre-reinforced high-performance concrete deep beams with and without openings, Materials (Basel), vol. 12, no. 1, 2018, doi: 10.3390/ma12010101.
[18] Dang TD, Tran DT, Nguyen-Minh L, Nassif AY. Shear resistant capacity of steel fibres reinforced concrete deep beams: An experimental investigation and a new prediction model. Structures 2021;33(May):2284–300. https://doi.org/10.1016/j.istruc.2021.05.091.
[19] Chen B, Zhou J, Zhang D, Su J, Nuti C, Sennah K. Experimental study on shear performances of ultra-high performance concrete deep beams. Structures 2022;39(March):310–22. https://doi.org/10.1016/j.istruc.2022.03.019.
[20] Sagar Varma Sagi M, Lakavath C, Suriya Prakash S. Effect of steel fibers on the shear behaviour of Self-Compacting reinforced concrete deep Beams: An experimental investigation and analytical model. Eng Struct 2022;269(June):114802. https://doi.org/10.1016/j.engstruct.2022.114802.
[21] Hassan HF. Behaviour of hybrid deep beams containing ultra high performance and conventional concretes. Eng Technol J 2015;33(1):30–50.
[22] Hassan SA, Mhebs AH. Behaviour of high strength hybrid reinforced concrete deep beams under monotonic and repeated loading. Open Civil Eng J 2018;12(1).
[23] Saad, A. Y., & Rasheed, L. S. (2018, November). Bbehaviours of hybrid deep beams with RPC Layers in the tension region. In IOP Conference Series: Materials Science and Engineering (Vol. 433, No. 1, p. 012032). IOP Publishing.
[24] Q. M. Shakir and H. K. Hanoon, "Behaviour Of High-Performance Reinforced Arched- Hybrid Self-Compacting Concrete Deep Beams," vol. 18, no. 1, pp. 792–813, 2023.
[25] Shakir QM, Hannon HK. a Novel Hybrid Model of Reinforced Concrete Deep Beams With Curved Hybridization. J Teknol 2023;85(2):31–9. https://doi.org/10.11113/jurnalteknologi.v85.18703.
[26] Shakir QM, Hanoon HK. New models for reinforced concrete precast hybrid deep beams under static loads with curved hybridization. Structures Aug. 2023;54:1007–25. https://doi.org/10.1016/j.istruc.2023.05.084.
[27] Iraqi Specification No.45, "Natural Sources for Gravel that is used in concrete and construction. Baghdad; 1984.
[28] Shakir QM, Abd BB. Retrofitting of Self Compacting RC Half Joints with Internal Deficiencies by CFRP Fabrics. Jurnal Teknologi 2020;82(6):49–62.
[29] Park R. 1988. "Ductility Evaluation from Laboratory and Analytical Testing". Proceedings of the 9th World Conference on Earthquake Engineering, Tokyo-Kyoto, Japan, Vol. 8, pp. 605-616.
[30] Zhang Y, Zhang S, Deng M. Four-point bending tests of ECC: Mechanical response and toughness evaluation. Case Stud Constr Mater 2022;17:e01573.
[31] Vu NS, Bing L, Beyer K. Effective stiffness of reinforced concrete coupling beams. Eng Struct 2014;76:371–82.
[32] Naaman A, Jeong S., Structural ductility of concrete beams prestressed with FRP tendons", In: Proc. Second Int. RILEM Symp. (FRPRCS- 2) Non-Metallic Concr. Struct., Ghent, Belgium, pp 379– 86, 1995.
[33] Iraqi Specification No. 5, (1984)," Portland Cement", Baghdad.1984.